2007

An electrospray-based, ozone-free air purification technology

Gary Tepper
Virginia Commonwealth University, gctepper@vcu.edu

Royal Kessick
Sentor Technologies Incorporated

Dmitry Pestov
Virginia Commonwealth University, dpestov@vcu.edu

Tepper, G., Kessick, R., & Pestov, D. An electrospray-based, ozone-free air purification technology. Journal of Applied Physics, 102, 113305 (2007).

An electrospray-based, ozone-free air purification technology

Gary Tepper[a)]
Sentor Technologies, Inc., Glen Allen, Virginia 23059, USA
and Virginia Commonwealth University, Richmond, Virginia 23284, USA

Royal Kessick
Sentor Technologies, Inc., Glen Allen, Virginia 23059, USA

Dmitry Pestov
Virginia Commonwealth University, Richmond, Virginia 23284, USA

(Received 3 July 2007; accepted 5 October 2007; published online 5 December 2007)

A zero-pressure-drop, ozone-free air purification technology is reported. Contaminated air was directed into a chamber containing an array of electrospray wick sources. The electrospray sources produce an aerosol of tiny, electrically charged aqueous droplets. Charge was transferred from the droplets onto polar and polarizable species in the contaminated air stream and the charged contaminants were extracted using an electric field and deposited onto a metal surface. Purified air emerged from the other end of the chamber. The very small aqueous electrospray droplets completely evaporate so that the process is essentially dry and no liquid solvent is collected or recirculated. The air purification efficiency was measured as a function of particle size, air flow rate, and specific system design parameters. The results indicate that the electrospray-based air purification system provides high air purification efficiency over a wide range of particle size and, due to the very low power and liquid consumption rate, can be scaled up for the purification of arbitrarily large quantities of air. © *2007 American Institute of Physics*. [DOI: 10.1063/1.2818364]

I. INTRODUCTION

According to the American Lung Association's "State of the Air 2006" report published in April 2006, over half of the U.S. population lives in counties with unhealthful levels of air pollution and over 50×10^6 Americans suffer from chronic exposure to particulate pollution.[1] This problem is not unique to the U.S. and affects most industrialized regions of the world. The adverse health effects and associated medical costs of air pollution are well documented and include increased risk of cancer, respiratory and cardiovascular disease and decreased life expectancy.[2–5] The Environmental Protection Agency's Clean Air Act was amended in 1990 in an attempt to curb three major threats to the health of millions of Americans: acid rain, urban air pollution, and toxic air emissions.[6] In addition to regulatory efforts to control and reduce emissions at the source, numerous consumer products targeting the rapidly growing air purification market have been introduced in recent years.

Consumer air purification products for particulate removal are generally based on mechanical filtration or electrostatic precipitation.[7–12] Mechanical (e.g., High Efficiency Particulate Air (HEPA)) filters simply capture those particles unable to pass through the filter. However, the filters must be changed regularly and offer significant resistance to air flow resulting in relatively high pressure drops and noise levels. Electrostatic precipitators, on the other hand, employ a corona discharge to ionize air molecules. The ionized air molecules attach to air contaminants, which are removed through the application of an electric field. However, while electrostatic precipitators are quiet and do not require filter replacement, they do produce ozone (an environmental health hazard) as a by-product of the ionization process. Ozone production severely limits the usefulness and scalability of air purification systems based on electrostatic precipitation.

Air purification systems based on a recirculating shower of water droplets have been developed and these so-called "wet scrubbers" are used primarily in industrial settings because this approach is very energy intensive due to the need to collect and recirculate large volumes of liquid.[13] However, the volumetric flow rate of an aerosol process can be reduced dramatically by reducing the average diameter of the droplets into the nanoscale. Electrospray is one process capable of producing aerosolized droplets in this size range.[14–16]

Here we introduce an air purification technology based on tiny electrically charged aqueous droplets produced from an array of electrospray sources. Electrospray ionization is normally used in conjunction with mass spectrometry for applications in analytical chemistry.[14] In electrospray ionization mass spectrometry a solute is dissolved in a liquid solvent and the solution is "electrosprayed" from the tip of a charged capillary needle resulting in a plume of charged solvent droplets containing the dissolved solute. The initial diameter of an electrosprayed droplet depends on factors such as the solution conductivity and flow rate and is typically on the order of microns.[15,16] However, as the volatile solvent evaporates from the charged droplet, the surface charge density increases until the droplet becomes unstable, breaking into a cascade of smaller "daughter" droplets. This process, known as a Coulombic explosion, repeats and the daughter droplets get smaller in each generation.

Figure 1 is a photograph of a plume of droplets produced from a conventional electrospray capillary needle source. A high voltage is applied to the tip of a capillary needle con-

a)Electronic mail: gctepper@vcu.edu.

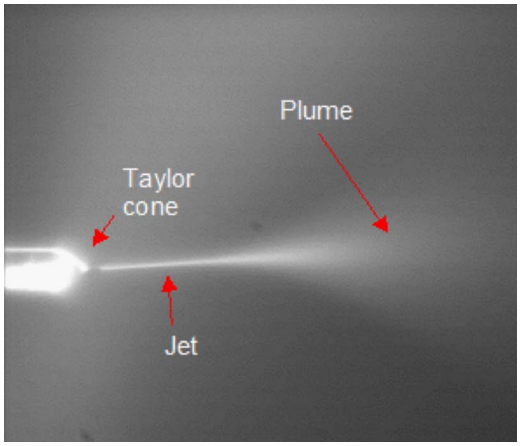

FIG. 1. (Color online) Photograph of an electrospray source illustrating the Taylor cone, jet, and plume.

taining an aqueous liquid. The electric field distorts the surface of the liquid and a characteristic Taylor cone is formed at the tip of the needle through a competition between surface tension and the applied electric force.[17] When the force from the electric field overcomes the surface tension, a charged liquid jet emerges from the tip of the Taylor cone and this is known as the cone-jet mode of electrospray. The jet eventually becomes unstable and breaks up into a plume or aerosol of tiny charged droplets. In this initial publication on the use of electrospray aerosols for air purification, no attempt will be made to present a detailed analysis of the electrospray hydrodynamics which has been described in detail in numerous publications including a very recent review.[17]

The charged nanodroplets produced in an electrospray process, if dispersed into the air, will transfer charge onto polar or polarizable species present in the air including both particles and polar molecules.[18] This article will focus on particle collection and the results of the vapor collection studies will be reported elsewhere. The charged nanodroplets interact with polar gas species through dipole-dipole interactions and will transfer charge onto polar or polarizable air contaminants without simultaneously ionizing the background, nonpolar nitrogen and oxygen air molecules (the primary components of air). This is an important part of the process because virtually all air contaminants such as odors, bacteria, dust, and pollen are polar or polarizable, while the normal components of air (nitrogen and oxygen) are nonpolar. Thus, it is possible to discriminate and convert all contaminants in an air stream into charged species, which can then be conveniently extracted and removed through the application of an electric field.

II. EXPERIMENTAL SECTION

The primary steps in the electrospray-based air purification process are illustrated in Fig. 2. Charged aqueous droplets were dispersed into an air stream using a plurality of electrospray wick sources. Charge was transferred from the fine mist of charged droplets onto any contaminants, but not onto the background air molecules. An electric field was then used to extract the charged contaminants from the incoming

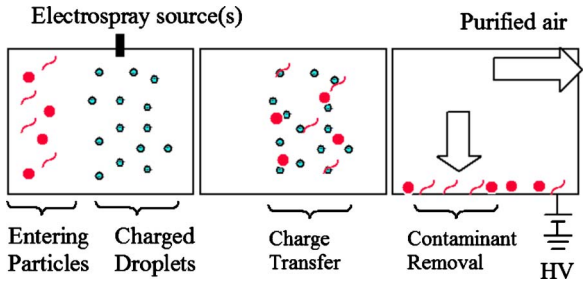

FIG. 2. (Color online) Schematic diagram illustrating the electrospray air purification process.

air stream. The purified air stream consisting of the uncharged nitrogen and oxygen molecules continues on unaffected by the charged droplets.

Two prototype air purification systems were constructed and tested. Wick-based electrospray sources were used in both systems instead of conventional capillary needles in order to eliminate the need for mechanical components such as syringe pumps, valves, or flow regulators. Once wet, the tip of the wick concentrates the electric field much like the tip of a hypodermic needle, while the body of the wick replenishes the electrospray solvent through capillary action as described by the Washburn equation.[19] A wick is also self-balancing in that it cannot provide solvent any faster than the electric field can remove it and the field cannot remove the solvent any faster than the wick can supply it. Finally, an array of wick sources can be used to conveniently distribute the electrospray aerosols over a large area for efficient and uniform contaminant ionization. Several different wick materials were tested including nylon, acrylic and a polyethylene/polyester blend from Porex. A more detailed analysis of these wick-based electrospray sources will be the subject of a separate publication.

Figure 3(a) is a schematic diagram illustrating the two main components of prototype A, which was constructed in a coaxial cylindrical geometry from PVC piping. Figure 3(b) is

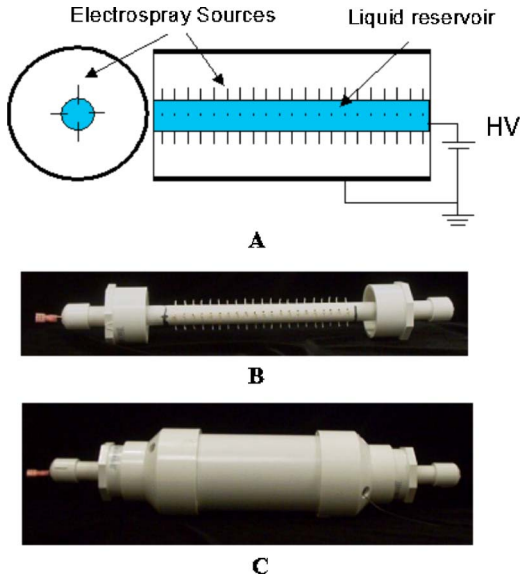

FIG. 3. (Color online) (a) Schematic diagram, (b) photograph of the wick array, and (c) fully assembled prototype A (cylindrical electrodes).

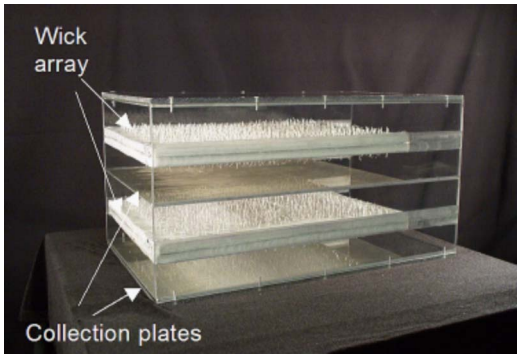

FIG. 4. (Color online) Photograph of prototype B (planar electrodes).

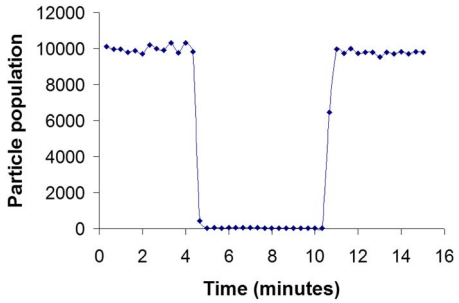

FIG. 5. (Color online) 0.3 μm particle population exiting the prototype A as the electrospray power is cycled ON and OFF at an air flow rate of 2.8 l/min.

a photograph of the inner cylinder containing the wick electrospray sources and Fig. 3(c) is a photograph of the fully assembled prototype A. The outer cylinder is 20 cm long with an inner diameter of 7.7 cm. The inner cylinder has a diameter of 2.1 cm so that the volume between the cylinders is approximately 0.86 l. 84 rigid Porex wick sources, 1 mm in diameter, were inserted through holes drilled into the inner PVC cylinder in four rows separated by 90 deg and directed radially toward the outer cylinder. This is a wick density of about 0.6 wicks/cm^2 or in terms of the volume of the chamber 98 wicks/l. Multiplexed electrospray sources have been reported in the literature for applications such as colloidal thrusters and mass spectrometry and while the close proximity of neighboring electrosprays must be considered when calculating the local electric field magnitude, the electrospray process has proven to be extremely robust to dense multiplexing.[20]

The tip of each wick was cut at an angle to provide a sharp edge and the bottom of each wick penetrated through the PVC wall and was in contact with a liquid reservoir inside the inner cylinder. The liquid consisted of 90% water and 10% ethanol. The purpose of the ethanol was to reduce the surface tension of the liquid to allow electrospray to initiate at a lower voltage than would be necessary for pure water. It is possible to electrospray from pure water but, due to the high surface tension of water, the voltage required to initiate an electrospray in water can be close to the air breakdown voltage.[21,22] The inner surface of the outer PVC cylinder was lined with aluminum and a small fan was used to direct air axially down the region between the two coaxial cylinders. A positive direct current (dc) voltage was applied to the liquid reservoir with respect to the grounded aluminum electrode on the inner surface of the outer cylinder. The magnitude of the dc voltage was an adjustable parameter, but was always maintained below 9 kV in order to prevent corona discharge. At voltages above 9 kV, this device became prone to corona discharge from the tip of some isolated wicks. The maximum electrospray current (at 9 kV) was about 10 μA or about 120 nA per wick, which is typical for an electrospray process. The total power consumption of the system, not including the fan, was about 0.09 W and the solvent consumption rate was on the order of 5 μl/min.

Figure 4 is a photograph of prototype B, which consists of four parallel-plate airflow channels inside of a clear plastic box with dimensions of 23 cm $\times$ 30 cm $\times$ 38 cm. Each airflow channel consists of a planar array of approximately 850 nylon wick electrospray sources on one side and a metal plate on the opposing side. The wick sources were arranged in equally spaced rows. The distance between the base of the wick array and the metal plate is between 4 and 5 cm and the total volume of the four parallel airflow channels is about 20 l. The wick density in prototype B was 170 wicks/l, which is nearly twice that of prototyope A. The soft nylon wicks were sewn into polyester reservoir pads into which the 90/10 water ethanol solvent was added until the pads became damp. Voltage was applied between each reservoir pad containing the electrospray wick sources and the grounded metal collecting plates. Multiple, parallel air flow regions were used in this design to increase the flow capacity without increasing the distance between the wick array and collecting electrode. The total power consumption of this larger prototype, not including the fan, was about 10 W and the total solvent consumption was estimated to be between 0.1 and 0.4 ml/min and depends on the air flow rate through the system which can strongly affect the liquid evaporation rate.

III. RESULTS

Ambient room air with a measured particle distribution was directed through prototype A using a "Sunon" fan mounted at the entrance port. The fan was run constantly and the flow rate into the cylindrical prototype was varied using a baffle. The air flow rate through the system was measured using a Bacharach Florite 800+ flow meter. A Handilaz miniparticle counter was placed at the exit and was used to measure the exiting particle population in comparison to the entering particle population for three particle sizes: 0.3, 0.5, and 5 μm. Figure 5 is a plot of the number of 0.3 μm diameter particles exiting prototype A as a function of time as the electrospray power is cycled on and off at an air flow rate of 2.8 l/min. The single pass air purification efficiency (defined as the entering minus the exiting particle count divided by the entering particle count) as a function of air flow rate at the three different particle sizes was measured and is shown in Fig. 6.

The air purification efficiency of prototype A was also measured as a function of applied voltage for the three different particle sizes at an air flow rate of 2.8 l/min. Figure 7 is a plot of the air purification efficiency as a function of applied voltage for these three different particle sizes.

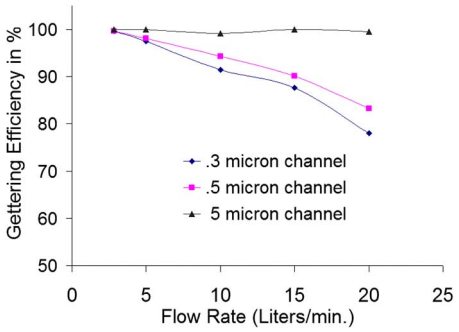

FIG. 6. (Color online) Air purification efficiency vs air flow rate for 0.3, 0.5, and 5.0 μm particles [electrospray prototype A operating at 9 kV (+)].

Prototype B was tested at Intertek Testing Services Corporation in Cortland, NY. The room air purification efficiency was tested for both cigarette smoke and dust. Prototype B was placed in the center of a small room with a room volume of approximately 1000 ft^3. Smoke or dust particles were dispersed into the room and a room fan was used to homogenize the particle distribution. A 200 cfm Hunter fan was used to send room air through the prototype and a particle counter, located within the room but not at the exit of prototype B, was used to sample the room air every 15 s over a period of 15 min.

Figure 8 is a plot of the room particle population versus time for smoke particles ranging in size from 0.065 to 1.0 μm. Figure 9 is a plot of the percent particle reduction after 15 min as a function of particle size. Between 75% and 90% of the smoke particles were removed from the room within 15 min with a minimum in the collection efficiency observed for particles with a diameter near 0.15 μm.

Figure 10 is a plot of the room particle population versus time for Arizona road dust particles ranging in diameter from 0.5 to 3 μm. The reduction in particle concentration over time with prototype B turned on is shown in comparison to the natural settling rate of these larger particles. Approximately 90% of the dust particles were removed from the room within 15 min.

IV. DISCUSSION

The data of Fig. 6 shows that the air purification efficiency of the cylindrical prototype A is higher for the large, 5 μm particles and, at the smaller particle sizes, decreases with increasing air flow rate. There is a substantial body of

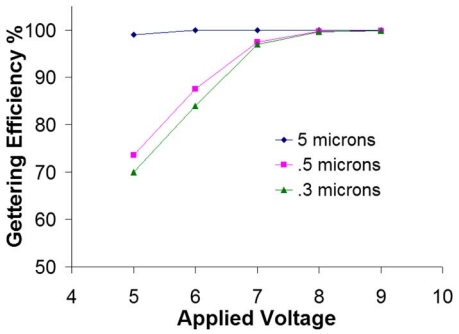

FIG. 7. (Color online) Air purification efficiency as a function of applied voltage for three particle sizes and an air flow rate of 2.8 l/min.

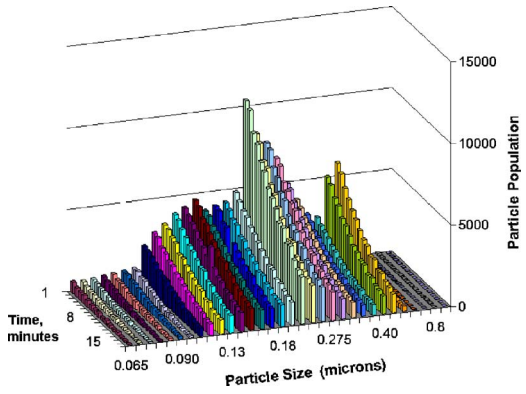

FIG. 8. (Color online) Plot of the particle population vs time for a 15 min test of prototype B. The particle size ranges from 0.065 to 0.9 μm and is for cigarette smoke.

literature on the mobility of charged particles in devices such as differential mobility analyzers (DMAs).[23–26] In the region between the two coaxial cylinders the electric field produced by the applied voltage is given by

$$E(r) = 1/r[V/\ln(R_2/R_1)], \tag{1}$$

where V is the applied voltage and R_1 and R_2 are the inner and outer radii of the cylinders, respectively. Ignoring the electric field distortions caused by the presence of the wicks and any space charge effects caused by the charged aerosol and assuming for the moment that the air flow pattern between the cylinders is axial and primarily laminar with a volumetric flow rate of Q (l/min), the minimum electrical mobility required for a positively charged particle originating near the entrance of the device and at the surface of the inner cylinder to traverse the radial distance to the outer cylinder just before being swept out of the device by the axial air flow is[23]

$$Z_{\min} = Q \ln(R_2/R_1)/2\pi LV, \tag{2}$$

where L is the length of the device. Unlike the particles in a DMA, the particles enter prototype A at various radial locations. Therefore, $Z_{\min}$ represents the minimum particle electrical mobility that is required for all entering particles to be removed from the air stream assuming instantaneous ionization (Fig. 11). However, radial motion toward the collector will not initiate until a particle becomes charged and, therefore, the collection probability for a given particle will depend both on the mobility of the particle as well as its ion-

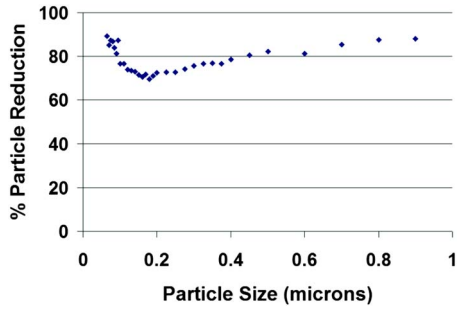

FIG. 9. (Color online) Percent particle reduction vs particle size over a 15 min test of prototype B. Particle population is for cigarette smoke.

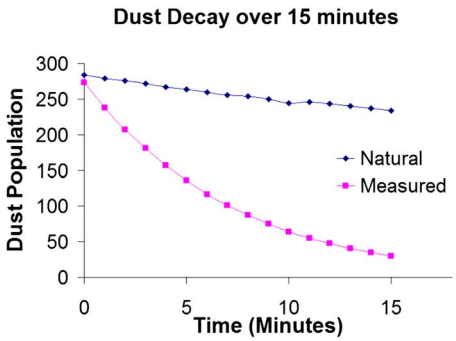

FIG. 10. (Color online) Plot of particle population vs time for Arizona road dust (particle size ranges from 0.5 to 3 μm). 15 min test of prototype B.

ization location within the device. The air purification efficiency, therefore, is obtained by integrating the collection probability over the distribution of particle mobilities and ionization coordinates. For example, if all particles enter the device with a single mobility equal to $Z_{\min}$ and are instantly ionized, the air purification efficiency in the absence of diffusion effects would be 100%. However, if ionization does not occur immediately and, for example, the particle trajectories originate uniformly throughout the device, the predicted air purification efficiency for particles with $Z=Z_{\min}$ drops to around 60%. This is because the fraction of particles that become charged within the volume downstream of the $Z_{\min}$ trajectory depicted in Fig. 11 will not be collected.

At a flow rate of 2.8 l/min and an applied voltage of 9000 V, $Z_{\min}=5\times10^{-5}$ cm^2/V s in prototype A. The actual particle electrical mobility Z_p depends on the particle diameter and the amount of charge and can be calculated from[23]

$$Z_p = nqC(D)/3\pi\mu D, \tag{3}$$

where n is the number of elemental charges on the particle, q is the magnitude of an elemental charge, μ is the gas viscosity (1.8×10^{-5} kg/m s for air at room temperature), and D is the particle diameter and $C(D)$ is the Cunningham correction factor. $C(D)$ depends on the particle diameter and approaches unity when the mean free path of a gas molecule is small in comparison to the particle diameter. The mean free path of an air molecule at atmospheric pressure is about 0.07 μm, which is significantly smaller than the smallest (0.3 μm) particles studied in prototype A. From Eq. (3) with $C(D)=1$, we determine the mobility of singly charged 0.3, 0.5. and 5 μm diameter particles as 3×10^{-5}, 2×10^{-5}, and 0.2×10^{-5} cm^2/V s, respectively.

From this mobility information, we can draw some qualitative conclusions from the experimental data of Figs. 6 and 7. The calculation predicts that the mobility of the 0.3 and 0.5 μm particles carrying a single unit of charge is just below $Z_{\min}$ at an air flow rate of 2.8 l/min (the lowest flow rate investigated). The measured air purification efficiency for these particles at this flow rate is close to 100%, and we conclude that most of the particle ionization must be occurring very close to the entrance of the device. As the flow rate is increased Eq. (2) predicts that the collection efficiency will drop off as seen in the data of Fig. 6. In addition, as the voltage difference between the inner and outer cylinders is decreased, $Z_{\min}$ increases and the collection efficiency would

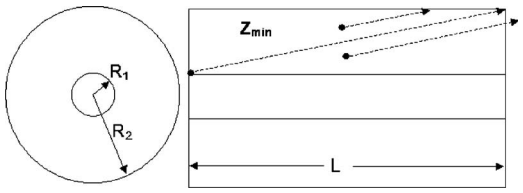

FIG. 11. Schematic diagram illustrating the minimum electrical mobility trajectory in the cylindrical prototype.

be expected to decrease as seen in the Fig. 7 data for the 0.3 and 0.5 μm particles. We conclude, therefore, that the 0.3 and 0.5 μm particles are most likely getting ionized very soon after entering the device and that the number of elemental charges deposited onto these submicron particles is low.

The mobility calculations for singly charged 5 μm particles do not correlate with the experimental collection efficiency data of Figs. 6 and 7. The experimental data show very high collection efficiency at flow rates as high as 20 l/min and voltages as low as 5 kV even though the mobility of these larger particles is much too small for them to traverse the distance between the inner and outer electrodes. We therefore conclude that the larger 5 μm particles are becoming multiply charged by the electrospray droplets, resulting in very high mobilities and the high collection efficiencies seen in the experimental data of Figs. 6 and 7. The propensity of the larger particles to become multiply charged is not unexpected and is due to their much larger radius. The saturation charge of a spherical particle in an electric field increases as the square of the radius as given by[27]

$$Q_{\max} = 4\pi\varepsilon_0 r^2 pE, \tag{4}$$

where E is the electric field magnitude and p is a parameter that is equal to 3 for conducting particles and is given by the following equation for dielectric particles:

$$p = 3\varepsilon_r/(\varepsilon_r + 2). \tag{5}$$

The earlier mobility calculations do not take into account the effects of the wick electrospray sources and assume both laminar flow as well as a purely radial electric field given by Eq. (1). The electric field magnitude in the vicinity of the wick sources will not follow Eq. (1) but will be enhanced due to the small radius of curvature. In addition, the electrospray plume will produce additional field distortions due to space charge effects. Also, the air flow pattern will be affected by the presence of the wicks and the electrospray aerosol which can trigger the onset of turbulence even at very low Reynolds numbers. Indeed, smoke visualization of the air flow patterns revealed some turbulent regions, particularly when the electrospray aerosols were on. Because of these complicating factors, the earlier mobility calculations must be considered qualitative in their predictive capabilities.

The single pass air purification efficiency for the larger prototype B was not measured. Instead the room air purification efficiency was determined for a 15 min operation cycle in order to relate this system to commercial products designed for room air purification. A Hunter fan with a flow rate of 200 cfm was used to direct air through the unit. At

this flow rate the air velocity is approximately 1.8 m/s, which corresponds to a particle residence time within the unit of about 0.2 s. A detailed analysis of the particle trajectories in prototype B would not be very informative at this time because we do not yet have single pass particle collection efficiency data for this device. However, the decay in room particle population over a 15 min test can be used to calculate a clean air delivery rate (CADR) number, which is used by the Association of Home Appliance Manufacturers (AHAM) as a common metric to quantify and compare the performance of commercial air purification systems.[28] As a rule of thumb, AHAM recommends selecting an air purification system with a CADR number at least 2/3 the square footage of the room. For a 10 ft$\times$12 ft room, for example, a CADR number of 80 or better is recommended. From the data of Figs. 8 and 9 the CADR number of prototype B was determined to be 104.5 and 136 for smoke and Arizona road dust, respectively. To our knowledge, this is one of the highest CADR numbers reported to date for a purely electrostatic device without any mechanical (e.g., HEPA) filtration. Therefore, we find that prototype B is ideally suited for the purification of room-size regions, but without ozone generation and with very low, nearly imperceptible, noise levels. The smaller prototype A would be more suitable for the purification of smaller volumes of air such as those required for a protective garment or mask. However, due to the simple modular design of prototype A, it is also possible to increase the air flow rate simply by operating multiple units in parallel.

In both prototypes the electrospray liquid completely evaporates and the grounded collecting electrodes remained dry during all of the tests. Therefore, no liquid collection or recirculation was necessary. Furthermore, the amount of power and liquid used was very small and, for example, at a liquid consumption rate of 0.1 ml/min (larger prototype B), 1 liter of liquid will last for up to 1 week under continuous operation and the power consumption is less than that of a single incandescent light bulb. We found that, due to the very low liquid consumption rate, the process did not significantly affect the background humidity in the room. Therefore, we conclude that room humidification is not an added benefit or detriment of this air purification technology.

In addition to air purification, the electrospray particle collection technology can be used as an efficient air sampler for the collection and analysis of aerosolized biological particles such as bacteria.[18] Electrospray is known to be a "soft," nondestructive ionization method and, therefore, would not be expected to kill or alter living organisms during ionization and collection.

We believe that the air purification efficiency of both prototypes can be significantly improved at all particle sizes by optimizing critical design parameters such as the number and spatial distribution of the wick sources as well as the electrospray solvent properties and the electrode spacing and configuration. The particle collection efficiency is a function of both the ionization probability and the particle mobility. Our results indicate that the particle mobility and not the ionization probability is the limiting factor at higher air flow rates. This suggests that the air purification efficiency can be increased either by increasing the length of the collection plates or by using a down stream impaction collector plate oriented perpendicular to the stream lines.

V. CONCLUSIONS

Ozone-free electrostatic precipitation systems based on an array of electrospray aerosols were developed and tested. The air purification efficiency was tested as a function of particle diameter, air flow rate and system design parameters. The electrospray-based air purification systems exhibit high particle collection efficiency over a broad distribution of particle sizes and may provide a healthy alternative to electrostatic precipitators based on corona discharge.

ACKNOWLEDGMENTS

This work was supported in part by the Defense Threat Reduction Agency under USARO Contract No. W911NF-06-C-0164. Initial charged droplet air sampling work was supported by the U.S. Army under STTR Contract No. W9132V-04-C-0023.

[1]The American Lung Association, State of the Air: 2006. See http://lungaction.org/reports/sota06_full.html.
[2]D. W. Dockery, C. A. Pope, X. P. Xu, J. D. Spengler, J. H. Ware, M. E. Fay, B. G. Ferris, and F. E. Speizer, N. Engl. J. Med. **329**, 1753 (1993).
[3]C. A. Pope, M. J. Thun, M. M. Namboodiri, D. W. Dockerty, J. S. Evans, F. E. Speizer, and C. W. Heath, Am. J. Respir. Crit. Care Med. **151**, 669 (1995).
[4]C. A. Pope III, R. T. Burnett, M. J. Thun, E. E. Calle, D. Krewski, K. Ito, and G. D. Thurston, J. Am. Med. Assoc. **287**, 1132 (2002).
[5]J. M. Samet, F. Dominici, F. C. Curriero, I. Coursac, and S. L. Zeger, N. Engl. J. Med. **343**, 1742 (2000).
[6]Environmental Protection Agency, Clean Air Act. See http://www.epa.gov/air/caa/.
[7]D. W. Hacker and E. M. Sparrow, Indoor Air **15**, 420 (2005).
[8]K. A. Adal, A. M. Anglim, C. L. Palumbo, M. G. Titus, B. J. Coyner, and B. M. Farr, N. Engl. J. Med. **331**, 169 (1994).
[9]S. K. Chen, D. Vesley, L. M. Brosseau, and J. H. Vincent, Am. J. Infect. Control **22**, 65 (1994).
[10]V. J. Novick, P. R. Monson, and P. E. Ellison, J. Aerosol Sci. **23**, 657 (1992).
[11]A. Mizuno, IEEE Trans. Dielectrics Electr. Insul. **7**, 615 (2000).
[12]G. Mainelis, S. A. Grinshpun, K. Willeke, T. Reponen, V. Ulevicius, and P. J. Hintz, Aerosol Sci. Technol. **30**, 127 (1999).
[13]K. C. Galbreath and C. J. Zygarlicke, Environ. Sci. Technol. **30**, 2421 (1996).
[14]J. B. Fenn, M. Mann, C. K. Meng, S. F. Wong, and C. M. Whitehouse, Science **246**, 64 (1989).
[15]K. Ichiki and S. Consta, J. Phys. Chem. B **110**, 19168 (2006).
[16]A. Gomez and K. Q. Tang, Phys. Fluids **6**, 404 (1994).
[17]J. F. de la Mora, Annu. Rev. Fluid Mech. **39**, 217 (2007).
[18]G. Tepper, J. Fenn, R. Kessick, D. Pestov, and J. Anderson, IEEE-Nano 2006, 2, 781 (2006).
[19]E. W. Washburn, Phys. Rev. **17**, 273 (1921).
[20]R. Bocanegra, D. Galan, M. Marquez, I. G. Loscertales, and A. Barrero, J. Aerosol Sci. **36**, 1387 (2005).
[21]J. M. Lopez-Herrera, A. Barrero, A. Booucard, I. G. Loscertales, and M. Marquez, J. Am. Soc. Mass Spectrom. **15**, 253 (2004).
[22]F. W. Peek, *Dielectric Phenomena in High Voltage Engineering* (McGraw-Hill, New York, 1929).
[23]E. O. Knutson and K. T. Whitby, J. Aerosol Sci. **6**, 443 (1975).
[24]R. C. Flagan, Aerosol Sci. Technol. **30**, 556 (1999).
[25]J. Rosell-Llompart, I. G. Loscertales, D. Bingham, and J. F. de la Mora, J. Aerosol Sci. **27**, 695 (1996).
[26]S. H. Kim, K. S. Woo, B. Y. H. Liu, and M. R. Zachariah, J. Colloid Interface Sci. **282**, 46 (2005).
[27]M. M. Pauthenier and M. Moreau-Hanot, J. Phys. Radium **3**, 590 (1932).
[28]Association of Home Appliance Manufacturers. See www.aham.org.